Pergamon

Cement and Concrete Research, Vol. 28, No. 8, pp. 1179–1190, 1998

0008-8846/98 $19.00 + .00

PII S0008-8846(98)00075-1

EFFECT OF MICROSTRUCTURE ON THE MECHANICAL AND THERMAL PROPERTIES OF LIGHTWEIGHT CONCRETE PREPARED FROM CLAY, CEMENT, AND WOOD AGGREGATES

A. Bouguerra,* A. Ledhem,* F. de Barquin,† R.M. Dheilly,‡ and M. Quéneudec‡
*Université de Rennes 1, IUT de Rennes 1, B.P. 1144, 3, rue du Clos Courtel, 35014 Rennes Cédex, France
†Centre Scientifique et Technique de la Construction, Division Matériaux, Av. Pierre Holoffe 21, 1342 Limelette, Belgique
‡Laboratoire Bâtiment:Université de Picardie Jules Verne, IUT, Département Génie Civil, Avenue des Facultés, Le Bailly, 80025 Amiens Cédex 01, France

(Received December 2, 1997; in final form May 11, 1998)

ABSTRACT

Wood concretes of a clayey matrix are considered herein from the standpoint of developing insulation materials through reliance on local resources and reusing industrial mineral wastes. Both the mechanical and thermal properties of these materials depend heavily on their microstructure and, in particular, on their porous structure which the authors have identified initially. An experimental study of the compression resistance as well as of the thermal conductivity in the dry state and at ambient temperature shows the changes in these characteristics as a function of porosity. A comparison with theoretical models previously tested for other types of cellular materials has served to validate its application in the case of wood concretes of a clayey matrix. © *1998 Elsevier Science Ltd*

Introduction

The term wood concrete indicates a composite material generally composed of a mineral matrix, possibly an admixture, and vegetable aggregates. These plant-based aggregates exhibit a grading comparable to that of conventional aggregates, yet with lower aggregate limits in the case of coarser aggregates. The standard matrices used are Portland cement mortars as well as magnesium cements, plaster and lime (1). In France, for a variety of reasons and technical requirements, the appearance of new lightweight concretes, in addition to the progress being made in both coatings and insulation materials, has limited the development of wood concrete in spite of attempts to promote its applications and to raise the public's awareness of environmental protection issues. Wood is, in fact, an entirely renewable resource and source for aggregates, especially so when prepared from perennials such as hemp (2). The basic arguments against the use of wood concretes are the irregularity of

[1]To whom correspondence should be addressed.

the concrete setting times and the poor adaptation to dimensional variations in existing coatings; these points have tended to outweigh the potential advantages associated with the lightness of the product, its thermal and acoustic qualities and the resultant productivity gains. The idea of using clayey materials in the composition of the matrix has recently been developed by various authors (3). This approach was reinforced by the conclusions drawn during the Second International Research Seminar on Local Building Materials, which emphasised the necessity of designing insulation materials using local resources (4). It has also been influenced by the need to valorize clayey co-products.

A material's macroscopic properties are closely linked to its porosity. The porosity of wood concretes stems from several sources. First of all, the water not used in the hydration of the cement evaporates, thus giving porosity to the matrix. This phenomenon is in reality a complex one, due to moisture exchanges in both the matrix and the wood aggregates which themselves are due to the porous structure. Furthermore, in certain compositions, the cause of porosity could be either the lack of mortar necessary to fill the space between the wood aggregates piled randomly or the phenomenon of a shrinkage of the matrix/aggregate interface. This wood concrete is therefore a complex porous structure which must be accurately identified before studying its relationship with respect to both mechanical and thermal properties.

Experimental Setup

Materials

The clayey fines used in this work are almost exclusively composed of kaolinites. Their absolute density, as measured by water pycnometry, is 2.65 g/cm^3, and the Atterberg limits reveal that the clayey material is somewhat malleable (5). The cement used is CPA CEM I 52.5 (EN 196–1). The aggregates are commercialised Picea wood aggregates of between 3 and 8 mm which have undergone both thermal and physical-chemical treatments. These treatment procedures do not affect the macroporosity of the wood aggregates.

Samples and Preparation of Test Specimens

The influence of the various components has already been studied (6). These results are to be acknowledged herein; for the purposes of this study, the following proportions of solid phases will be systematically used: cement = 25%, and clay + wood aggregates = 75% (see Table 1). In order to control moisture, the materials are initially dried. Dry mixing is essential in obtaining a truly homogenised mixture. The fines and cement are introduced into a planetary-movement mixer and subsequently mixed at low speed for 3 min. Wood aggregates are then added to the perfectly-homogenised mixture while keeping the mixer at low speed for another 3 min. The quantity of water was calculated to obtain the same level of workability for all the mixtures and is given by the following empirical relationship (6):

$$\text{Water (L)} = 0.45\,(Cl + C) + 0.8\,WAs \quad (1)$$

where C is the cement weight (kg); Cl is the clay weight (kg); and WAs is oven-dry wood aggregates (kg).

Water is added gradually throughout the entire mixing stage. Homogenisation is guaran-

TABLE 1
Mix proportions and densities of materials studied.

Relative mass fraction of wood aggregates $WA/(WA + Cl)$ (%)	Clay (*Cl*) (by mass)	Cement (*C*)	Wood aggregates (*WAs*) (by mass)	Density $g \cdot cm^{-3}$
0%	75.0	25.0	0.0	1.283
10%	67.5	25.0	7.5	1.065
20%	60.1	25.0	14.9	0.908
25%	56.2	25.0	18.8	0.862
30%	52.4	25.0	22.5	0.800
35%	48.5	25.0	26.5	0.728
40%	45.0	25.0	30.0	0.681
50%	37.5	25.0	37.5	0.621

teed by low-speed mixing for 3 min. followed by high-speed mixing for 1 min. After mixing, the material is placed in the moulds. The mixture is poured into the moulds while ensuring that air bubbles are not trapped in the fresh mixture. The excess in the mixture is then removed by levelling. The filled moulds are kept in a hygrometric and temperature-controlled room (at 20°C and 95% relative humidity). Samples are removed from the moulds one day after fabrication and then placed in a storage room for 28 days. The resulting densities are also presented in Table 1.

Measurement Apparatus

An analysis of the porosity has been conducted using a variety of techniques. Total porosity was determined by mercury porosimetry (Auto-Pore III 9400 from the Micrometrics Corp.) and by saturation in a vacuum, in compliance with the RILEM recommendations (7). An identification of the pore size distribution was also carried out using mercury porosimetry on samples of 10 mm $\times$ 10 mm $\times$ 20 mm in size. Equipment requirements have necessitated that the samples be sized at the limit of the range of representativity with respect to the dimensions of the wood aggregates. In order to correct this problem, three randomly-chosen samples were used and their composition has been studied. The results given below represent the averages of the measurements taken. The mechanical resistance values were determined on similar-shaped samples using a 20-kN capacity Walter Baibag press. The thermal conductivity was determined with the help of a thermal probe of weak inertia (8) on the previously described samples.

Experimental Results and Analysis

Pore Structure Parameters

The measured values of total porosity obtained by various methods are reported in Table 2. The determination of the mercury porosimetry can pose problems if the pressure applied does

TABLE 2
Total porosity, comparison between different methods.

Relative mass fraction of wood aggregates $WA/(WA + Cl)$ (%)	Mercury intrusion porosimetry (%)	Saturation under vacuum (%)	Calculated from mix proportions (%)
0	48.49	52.15	49.80
10	54.58	54.58	56.64
20	62.08	61.16	61.35
25	63.58	64.72	63.31
30	64.89	65.89	64.96
35	66.00	66.92	66.48
40	67.70	67.61	67.68
50	70.38	70.45	69.79

not fill all of the pores. In addition, the micropores are not accessible by mercury porosimetry. However, Table 2 shows that the results obtained using various techniques are very similar, which leads us to suppose both that the quasi-totality of the porosity has been explored and that the proportion of pores less than 2nm in size is relatively small. The variation in total porosity as a function of the wood's mass content is represented in Figure 1. It should be noted that this variation can be represented by a second-order polynomial law as a function of the mass content of the wood aggregates, with a suitable correlation coefficient. Finally, the measured values using mercury porosimetry and the calculated values using the various proportions of the constituents exhibit a strong level of agreement (5) (Table 2).

Pore-Size Distribution

The determination of the pore-size distribution is measured by evaluating the mercury penetration in the cavities. However, some imprecision remains with respect to the connectivity existing between various-sized pores (9). To reach pores of a given characteristic size,

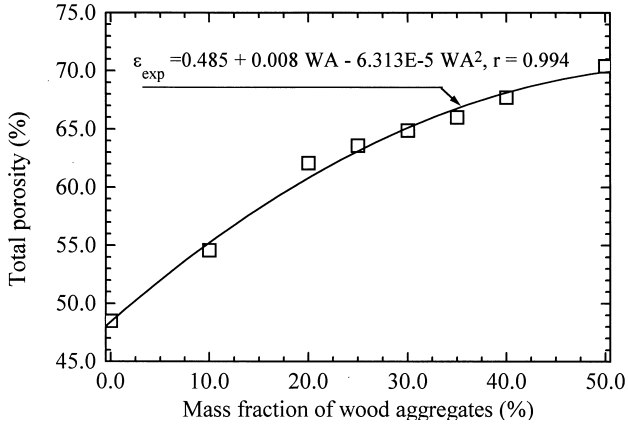

FIG. 1.
Variation of total porosity as a function of the mass fraction of wood aggregates.

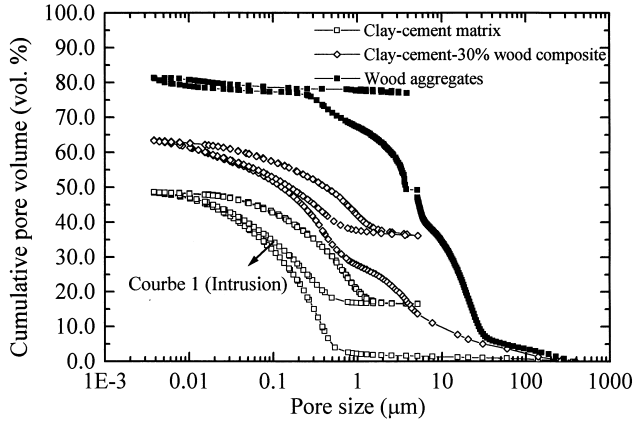

FIG. 2.
Pore size distribution curves of clay-cement matrix, clay-cement-30% wood composite, and wood aggregates, respectively.

it is necessary to cross the apertures with a smaller size (ink-bottle pores), and the volume of the cavity being taken into account will then correspond to the sum of those pores whose characteristic size is equal to that of the entry pore (10). The mercury porosimetry leads to a systematic overestimation of the volume and surface area of the finest pores, to the detriment of the widest, without making it possible to evaluate their relative proportions. In addition, the entrapment of mercury in certain pores during the repeated cycles forms a hysteresis whose surface and shape depend on the following pore structure characteristics: the quantity of ink-bottle pores, the mean pore to throat ratio, the pore connectivity and surface roughness of the pores which can lead to a change in the mercury contact angle between intrusion and extrusion. Nevertheless, the interpreting of the hysteresis effect in terms of a quantitative pore description is very difficult, and many research actions are still made on the subject (11). The most significant parameter that we can get out of this hysteresis is given by its lowest point, i.e., the quantity of mercury being trapped in the sample at atmospheric pressure. Expressed relatively to the total porosity, this parameter is called “entrapped porosity”. It gives an estimation of the percentage of large pore cavities in the sample, which can be considered as non-capillary pores. We observe in Figure 2 that the value of the entrapped porosity increases with the relative quantity of wood aggregates in the samples. Mercury porosimetry on the wood aggregates alone shows a flat desorption curve. This is due to the fact that pores in wood are too large to be drained at atmospheric pressure. Theoretically, a gradual depression should be made on the sample to see the complete desorption curve but in practice this operation is not allowed with the used porosimeter.

In this work, we are essentially interested in the curve of the first intrusion. Figure 3 displays the accumulated normalised volume, i.e., the ratio of the cumulative volume to the total porosity as a function of the average diameter of the pores. The contact angle in both intrusion and extrusion is 142°. It should be pointed out that the mesopores and the macropores vary in a proportion of 2:4 between the two limits of the percentage variance (0 to 30%, respectively) of wood aggregates.

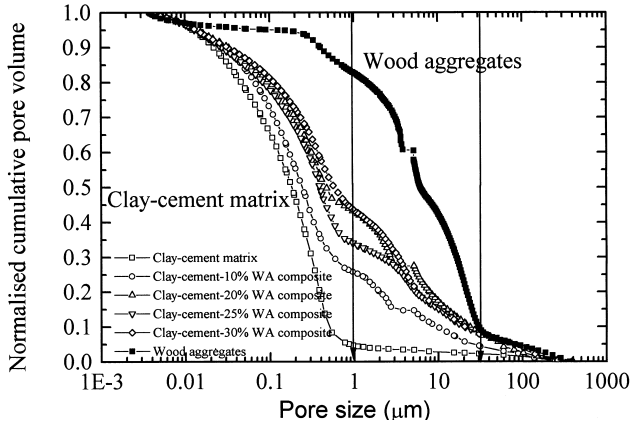

FIG. 3.
Normalised cumulative pore volume for clay-cement matrix and clay-cement-wood aggregates composite for various percentages of wood aggregates.

Structure of Composite

Moreover, in order to verify that this macroporosity is due to the structure of the wood aggregates themselves and not to the porosity problems induced by either the entry of air, the fissuring of the matrix, or the matrix/aggregate interface, a microscopic study has been undertaken. The homogeneity of the matrix was verified using an optical microscope and a scanning electronic microscope: see Figures 4 and 5. Figures 6 and 7 show the matrix/wood aggregate adherence under both an optical microscope and a scanning electronic microscope for 10% to 20% of wood aggregates, respectively. In addition, an examination of the matrix under an optical microscope reveals a homogeneous and compact microstructure. We have deduced from this identification of the porous structure that wood concretes of a clayey matrix are complex porous composites in which the macroporosity ($\Phi > 1$ μm) is generated

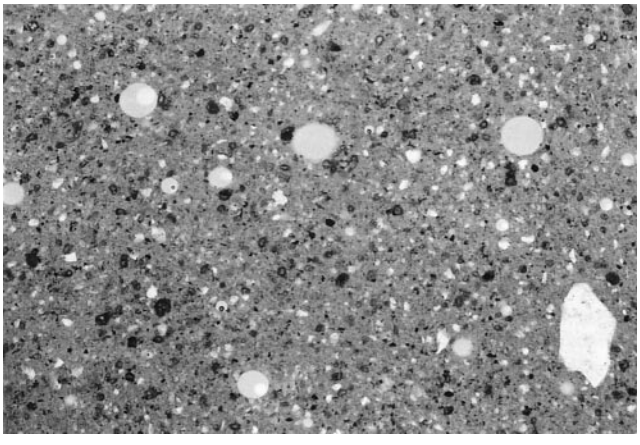

FIG. 4.
Optical micrograph of clay-cement matrix (10×) (65 days).

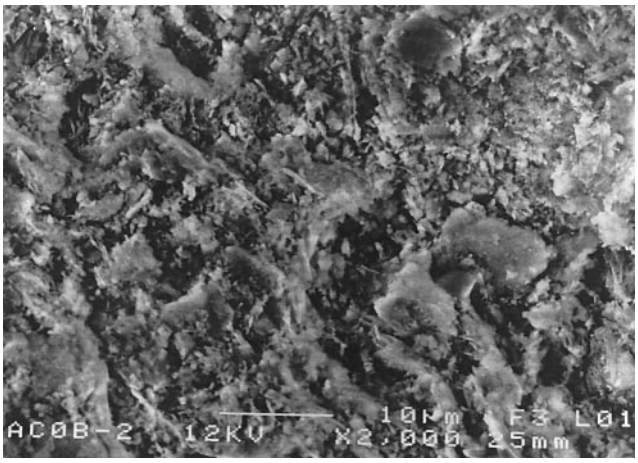

FIG. 5.
SEM observation of microstructure of clay-cement matrix (2000×) (365 days).

by the wood aggregates and the localised mesoporosity (2.10^{-3} μm $< \Phi <$ 1 μm) is essentially in the matrix. The microporosity ($\Phi < 2.10^{-3}$ μm) is almost non-existent. In the following sections, we shall try to relate this porosity to the mechanical and thermal characteristics of the materials in a dry state.

Relationship to Mechanical Properties

Many relationships, based on experimental data, between compressive strength and porosity have been forwarded. A complete review of these relationships can be found in (12–25). The four basic types of equations that are generally used are listed in Table 3.

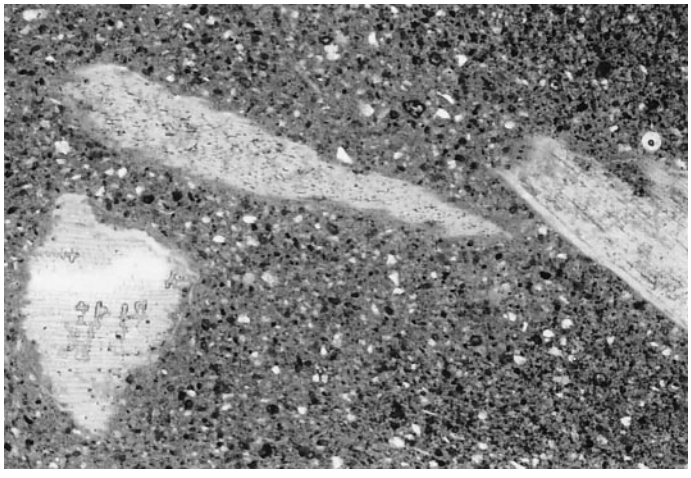

FIG. 6.
Optical micrograph of the matrix-wood aggregates bound (10×) (65 days).

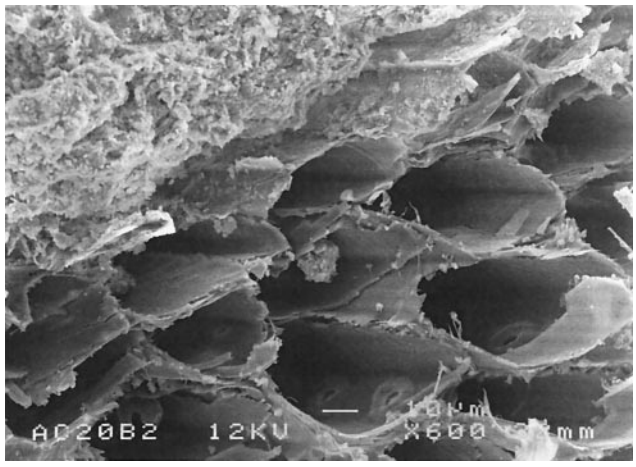

FIG. 7.
SEM micrograph of clay-cement-20% wood aggregates (600×) (365 days).

In this work, these various relationships were compared with experimental results obtained for wood concretes with a clayey matrix. The variation in the compressive strength derived experimentally from total porosity is given in Figure 8. Note should be made of the rapid decrease, which is probably due to the increase in the macroporosity as the total porosity increases. The theoretical curves resulting from the use of various models are also presented in the same figure. We have tried to optimise the values of the different constants; these results are reported in Table 4. The coefficients were calculated by regression on the experimental curve. The corresponding correlation coefficients exhibit a strong level of agreement between expressions, along with the experimental results obtained for a total porosity of between 0.5 and 0.7. However, if we were to consider the values derived for σ_{c0} by these different laws, we would recognise that the values are actually dispersed. The Ryshkewitch expression yields an overvaluation of σ_{c0}. This result serves to confirm Niels-

TABLE 3
Equations for the strength-porosity relationship of clay-cement-wood aggregates composite.

Model	Empirical equation
Bal'shin (12)	$\sigma_c = \sigma_{c0}(1 - n)^m$
Ryshkewitch (13)	$\sigma_c = \sigma_{c0} \exp(-m \cdot n)$
Schiller (14)	$\sigma_c = \sigma_{c0} \ln(n/n_o)$
Hasselman (15)	$\sigma_c = \sigma_{c0} - m \cdot n$

σ_c is the strength of the porous material, σ_{c0} the theoretical strength of the material at zero porosity, n the porosity, n_0 the critical porosity corresponding to zero strength, and m an empirical constant.

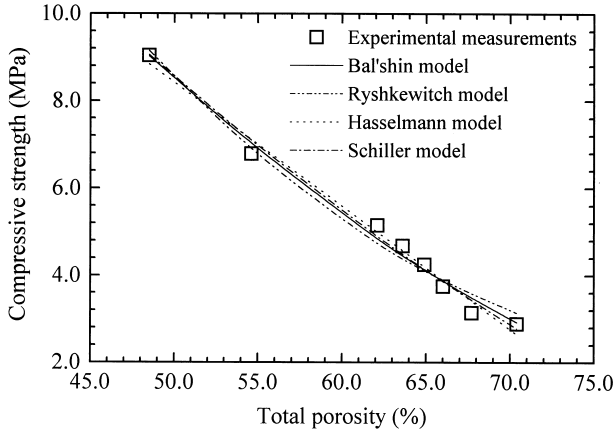

FIG. 8.
Comparison between of experimental results with calculated compressive strength for clay-cement-wood aggregates composite.

en's conclusions (25). Furthermore, as previously noted by the author, the Bal'shin and Hasselman models are better adapted for relating compression resistance to total porosity.

Relationship to Thermal Conductivity

Wood-clay-cement composites are materials exhibiting a double porosity, whereby the mesoporosity is essentially localised in the clay-cement matrix. The macroporosity results from the wood aggregates. In order to predict the thermal conductivity at lower temperatures of the clay-cement- wood-aggregate composite, we have considered the composite as constituted by the porous binder matrix, i.e., clay and hydrated cement paste and wood aggregates. On the other hand, a composite is considered as containing inclusions embedded in a matrix material. From among the various models proposed in the literature on predicting the thermal conductivity of porous materials, a modified unit cell of a parallel model has been used. A detailed description of this conceptual model has been presented in a previous paper (26). This model, in addition to including the characteristics of different phases, such as the thermal conductivity of each phase and the phase's volumic fraction, takes into account the geometry of the pore structure by introducing a morphological parameter such as a tortuosity. This model distinguishes also between microporosity and macroporosity and considers the

TABLE 4
Parameters and correlation coefficients of different models.

Model	σ_{c0}	m	r
Bal'shin	34.836	2.046	0.9943
Ryshkevitch	97.778	4.884	0.9899
Schiller	0.830	0.0594	0.9943
Hasselmann	22.568	−28.296	0.9953

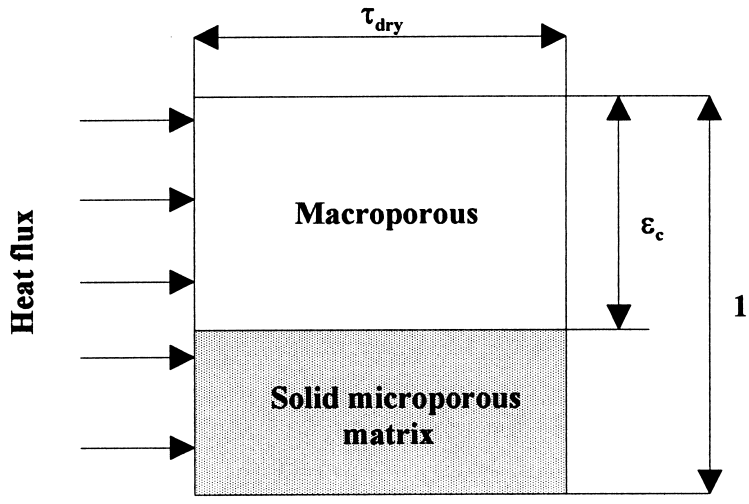

FIG. 9.
Unit cell of parallel model for the estimation of thermal conductivity at dry state.

internal structure of the material as a dispersion of macropores in a homogeneous solid microporous matrix. Two structural parameters have been introduced to describe the unit-cell model: the "tortuosity" factor τ and the rate of macroporosity ϵ_χ, which can be defined as the percentage of macro-voids within the material. The representative unit of such a structure is shown in Figure 9

The apparent heat flux through a composite is the sum of the flux through the solid part and the flux through the macro-void part. Thus, the effective thermal conductivity at both low temperatures and dry state can be expressed as:

$$\lambda_{dry} = \frac{(1 - \varepsilon_c) \cdot \lambda_{sm} + \varepsilon_c \lambda_{air}}{\tau_{dry}} \tag{2}$$

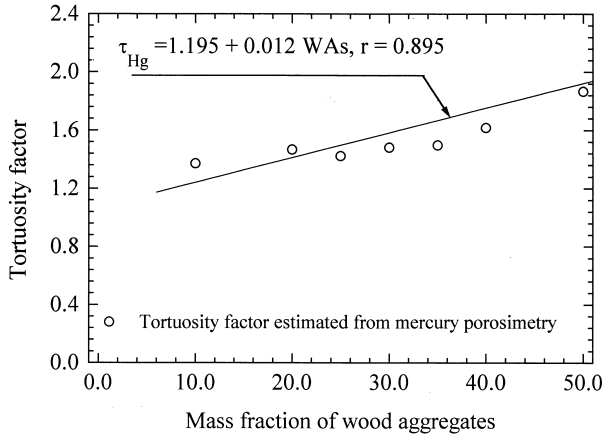

FIG. 10.
Variation of tortuosity factor estimated from mercury intrusion porosimetry.

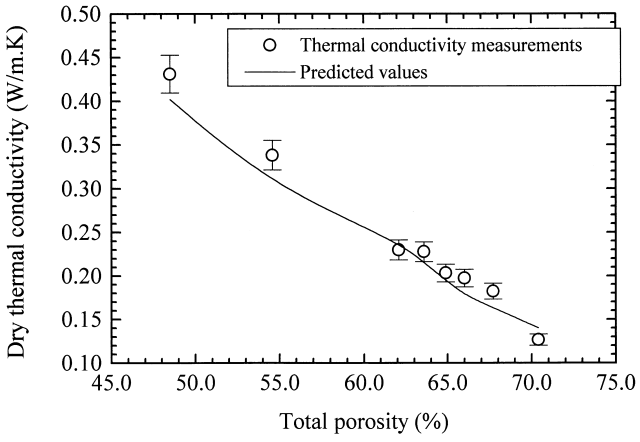

FIG. 11.
Comparison between measurement thermal conductivity using thermal probe technique and predicted thermal conductivity using a modified unit cell of parallel model.

where λ_{sm} is the thermal conductivity of the solid microporous matrix (0.4321 W/m.K), i.e., the reference mixture (clay-cement matrix) without wood aggregates; λ_{air} the thermal conductivity of air; and τ_{dry} the "tortuosity" factor at the dry state which takes into account the deviation of heat flux lines due to the wood aggregates.

The "tortuosity" factor at the dry state has been calculated from mercury porosimetry (27) (Fig. 10). It can thus be seen that the "tortuosity" factor increases as the percentage of wood aggregate increases. This can be interpreted from the fact that because the particles of wood aggregates are randomly distributed within the solid microporous matrix, the direction of the flux lines is changed upon each encounter with these particles. Therefore, when the amount of wood aggregate increases, the path of the flux lines becomes more tortuous. The rate of macroporosity is equal to the rate being exhibited by the wood aggregates (5).

Figure 11 shows the variation in thermal conductivity estimated from equation (2) at the dry state by percentage of wood aggregate. The results obtained from the proposed model strongly agree with experimental measurements. It is worth noting that the percentage error between theoretical and experimental results using the parallel model lies between 4% and 10%.

Conclusions

In this paper, the influence of the pore structure of lightweight concrete, obtained from clay, cement and wood aggregates, on both mechanical and thermal properties has been investigated. From the results described above, the following set of conclusions can be drawn:

1. A microstructural analysis undertaken on the basis of Mercury Intrusion Porosimetry has shown the effect of macro-sized wood aggregates on the pore-size distribution of the studied materials. As the mass content of the wood aggregates increases, the proportion of macropores also increases.
2. A comparison between the measured values of total porosity obtained with the Mercury Intrusion Porosimetry method and those obtained with the vacuum-saturation method

using water has demonstrated that the quasi-totality of the porosity had been examined and that the proportions of micropores are nil.

3. Images from both a scanning electron microscope and an optical microscope have revealed a homogeneous and compact microstructure of the clay-cement matrix along with a very strong matrix-wood aggregate bound. This finding serves to confirm that the macroporosity is generated by the wood aggregates and the localised mesoporosity is essentially in the matrix.
4. The results of the compressive strength tests indicate that the wood aggregate-clay-cement composites satisfy the requirements for both primary and secondary construction applications, depending on the mass content of the wood aggregates. A very strong level of agreement has been observed between the predicted values of compressive strength as derived from four models proposed by different authors and the experimental measurements.
5. Wood aggregates greatly improve the thermal conductivity of the composite. A theoretical model using the concept of tortuosity, which had already been validated for other materials, was used for calculating the thermal conductivity of a wood aggregate-clay-cement composite. A study using this model has demonstrated the effect of porosity on thermal conductivity. It has been shown that the thermal conductivity of lightweight concrete changes considerably with porosity.

References

1. P. Pimenta, J. Chandelier, M. Rubaud, F. Dutruel, and H. Nicole, Cahiers du CSTB 346, 1 (1994).
2. P. Sionneau, F. Périer, M. Quéneudec, and A. T'kint de Roodenbeke, Revue Internationale d'Héliotechnique 9, 12 (1994).
3. A. Bouguerra, A. Ledhem, and M. Quéneudec, Proceedings of Conchem Conference Bruxelles, p. 483, 1995.
4. RILEM Bulletin, Recherche sur les matériaux locaux, Mater. Struct. 29, 190 (1996).
5. A. Bouguerra. Lyon, France: INSA de Lyon; Ph.D. Thesis. 1997.
6. K. Al Rim. Rennes, France: Université de Rennes; Ph.D. Thesis. 1994.
7. RILEM, CPC 11.3, Mater. Struct. 17, 391 (1984).
8. J.P. Laurent, Int. J. Heat Mass Transfer, 32, 1247 (1989).
9. H.W. Reinhardt and K. Gaber, Mater. Struct., 23, 3 (1990).
10. F. Metz, and D. Knöfel, Mater. Struct., 25, 127 (1992).
11. H. Giesche, Proc. of Mater. Res. Soc. Symp. 431, 251 (1996).
12. M.Y. Balshin, Dokl. Akad. Nauk. SSSR 67, 831 (1949).
13. E. Ryshkewitch, J. Amer. Ceram. Soc. 36, 65 (1953).
14. K.K. Schiller, Brit. J. Appl. Phys. 11, 338–342 (1960).
15. D.P.H. Hasselman, J. Amer. Ceram. Soc. 46, 564 (1963).
16. S. Mindess. Stanford University; Ph.D. Thesis. 1970.
17. S. Mindess, Proc. Mater. Res. Soc. Symp., Boston, Mass. 53 (1984).
18. D.M. Roy and G.R. Gouda, J. Amer. Ceram. Soc. 56, 549 (1973).
19. D.M. Roy, G.R. Gouda, and A. Bobrowsky, Cem. Concr. Res. 2, 349 (1972).
20. H. Rössler and I. Odler, Cem. Concr. Res. 15, 320–330 (1985).
21. M. Yudenfreund, I. Odler, and S. Brunauer, Cem. Concr. Res. 2, 313 (1972).
22. K.L. Watson, Cem. Concr. Res. 11, 473 (1981).
23. D.G. Manning and B.B. Hope, Cem. Concr. Res. 1, 631 (1971).
24. J.J. Beaudoin, Cem. Concr. Res. 13, 81 (1983).
25. F.L. Nielsen, Mater. Struct. 26, 255 (1993).
26. J.P. Laurent, Mater. Struct., 24, 221 (1991).
27. S.C. Carniglia, J. Catalysis, 102, 401 (1986).